Journal of Zhejiang University SCIENCE A
ISSN 1673-565X (Print); ISSN 1862-1775 (Online)
www.zju.edu.cn/jzus; www.springerlink.com
E-mail: jzus@zju.edu.cn

Pressure observer based adaptive robust trajectory tracking control of a parallel manipulator driven by pneumatic muscles*

ZHU Xiao-cong†, TAO Guo-liang†‡, CAO Jian
(*The State Key Laboratory of Fluid Power Transmission and Control, Zhejiang University, Hangzhou 310027, China*)
†E-mail: zhuxiaoc@zju.edu.cn; gltao@zju.edu.cn
Received Mar. 6, 2007; revision accepted Aug. 1, 2007

Abstract: This paper presents a pressure observer based adaptive robust controller (POARC) for posture trajectory tracking of a parallel manipulator driven by three pneumatic muscles without pressure sensors. Due to model errors of the static forces and friction forces of pneumatic muscles, simplified average flow rate characteristics of valves, unknown disturbances of entire system, and unmeasured pressures, there exist rather severe parametric uncertainties, nonlinear uncertainties and dynamic uncertainties in modeling of the parallel manipulator. A nonlinear pressure observer is constructed to estimate unknown pressures on the basis of a single-input-single-output (SISO) decoupling model that is simplified from the actual multiple-input-multiple-output (MIMO) coupling model of the parallel manipulator. Then, an adaptive robust controller integrated with the pressure observer is developed to accomplish high precision posture trajectory tracking of the parallel manipulator. The experimental results indicate that the system with the proposed POARC not only achieves good control accuracy and smooth movement but also maintains robustness to disturbances.

Key words: Pneumatic muscle, Parallel manipulator, Pressure observer, Adaptive robust control, Trajectory tracking
doi:10.1631/jzus.2007.A1928 **Document code:** A **CLC number:** TH138

INTRODUCTION

A pneumatic muscle is a new kind of pneumatic actuator similar to human muscle, which has been gradually applied in robotic manipulators (Caldwell *et al*., 1995; Medrano-Cerda *et al*., 1995; Tondu and Lopez, 2000; Nakamura *et al*., 2002; Tsagarakis and Caldwell, 2003; Costa and Caldwell, 2006; Takuma and Hosoda, 2006; Ahn and Nguyen, 2007). The parallel manipulator driven by three pneumatic muscles studied in this paper has the advantages of cleanness, light weight, low cost, easy maintenance, compact structure and high power/volume ratio, and will have promising wide applications in robotics, industrial automation and bionic devices (Zhu and Tao, 2004; Tao *et al*., 2005).

Due to model errors of the static forces and friction forces of pneumatic muscles, simplified average flow rate characteristics of valves, and unknown disturbances of the entire system, there exist rather severe parametric uncertainties and nonlinear uncertainties in modeling of the parallel manipulator. Recently, an adaptive robust controller has been designed to effectively deal with the above uncertainties with the guarantee of good transient performance and final tracking accuracy (Zhu *et al*., 2006). In order to reduce cost and complexity of the pneumatic system, pressure sensors should be used as little as possible in practice. Therefore, it is necessary to develop this controller without the need of measuring pressures for trajectory tracking of the parallel manipulator driven by pneumatic muscles. However, the absence of pressure sensors will bring a new challenge for controlling such a system and achieving good performance since pressure feedback is really needed in the previous adaptive robust controller.

‡ Corresponding author
* Project (No. 50775200) supported by the National Natural Science Foundation of China

In recent years, many researchers have worked on applying observer theory to designing controller of pneumatic systems and cancelling pressure sensors. Specially, Hildebrandt *et al.*(2005) proposed a feedback linearization controller based on a pressure observer for tracking control of a pneumatic system, which is realized by parameterizing the chamber pressures in respect of the actual position and corresponding derivatives. Gulati and Barth (2005) presented a sliding mode controller based on either energy based or force-error based Lyapunov pressure observer for servo control of pneumatic actuators. Pandian *et al.*(2002) developed a continuous gain observer and a sliding-mode observer to estimate the pressures in the cylinder, and used the estimated pressure in a sliding-mode controller for tracking control of a pneumatic cylinder. For the parallel manipulator studied, it must be noted that the system has MIMO coupling dynamics and large uncertainties associated with the pneumatic muscle, and that the unmeasured pressure could not be accurately represented by other measured state variables in linear form. Therefore, the designing method of this pressure observer is different from those in the above literature.

In this paper, informed by research on the adaptive robust observer (Yao and Xu, 2001), a nonlinear pressure observer based on a simplified SISO decoupling model with large uncertainties, is integrated with an adaptive robust controller to accomplish high precision posture trajectory tracking of the parallel manipulator without the need of measuring pressures.

DECOUPLING DYNAMICS

The parallel manipulator driven by three pneumatic muscles (manufactured by Festo, MAS-40-N600-AA-MCKK) is shown in Fig.1, which consists of a moving platform, a base platform, a central pole and three pneumatic muscles connected by six ball joints that are evenly distributed along the respective platforms. The central pole is fixed to the base platform and is connected to the moving platform by a spherical joint. Two fast switching valves (manufactured by Festo, MHE2-MS1H-3/2G-M7-K, 100 L/min) are utilized to control the pressure inside each pneumatic muscle and this combination of components is referred to as a driving unit subsequently.

1: Moving platform; 2: Ball joint; 3: Spherical joint
4: Pneumatic muscle; 5: Central pole; 6: Base platform

Fig.1 Experimental test-rig of parallel manipulator driven by pneumatic muscles

SISO decoupling model in task-space

The dynamics in task-space of the parallel manipulator is given by (Zhu *et al.*, 2006; Tao *et al.*, 2007)

$$\boldsymbol{M}(\boldsymbol{\theta})\ddot{\boldsymbol{\theta}}+\boldsymbol{C}(\boldsymbol{\theta},\dot{\boldsymbol{\theta}})\dot{\boldsymbol{\theta}}+\boldsymbol{G}(\boldsymbol{\theta})+\boldsymbol{J}^{\mathrm{T}}(\boldsymbol{\theta})\boldsymbol{F}_{\mathrm{f}}(\boldsymbol{l},\dot{\boldsymbol{l}},\boldsymbol{p})+\boldsymbol{d}_{\mathrm{t}}(t) \\ =\boldsymbol{J}^{\mathrm{T}}(\boldsymbol{\theta})\boldsymbol{F}_{\mathrm{m}}(\boldsymbol{p},\boldsymbol{l}), \tag{1}$$

where $\boldsymbol{\theta}=[\theta_x,\theta_y]^{\mathrm{T}}$ is the posture vector of the parallel manipulator, $\boldsymbol{l}=[l_1,l_2,l_3]^{\mathrm{T}}$ is the contractive length vector of pneumatic muscles, $\boldsymbol{p}=[p_1,p_2,p_3]^{\mathrm{T}}$ is the relative pressure vector of pneumatic muscles, $\boldsymbol{M}(\boldsymbol{\theta})$ is the rotational inertial matrix, $\boldsymbol{C}(\boldsymbol{\theta},\dot{\boldsymbol{\theta}})\dot{\boldsymbol{\theta}}$ is the vector of centripetal and Coriolis torques, $\boldsymbol{G}(\boldsymbol{\theta})$ is the vector of gravitational torques, $\boldsymbol{F}_{\mathrm{f}}(\boldsymbol{l},\dot{\boldsymbol{l}},\boldsymbol{p})$ is the friction force vector of pneumatic muscles and link-joints, $\boldsymbol{d}_{\mathrm{t}}(t)$ is the disturbance vector in task-space, $\boldsymbol{J}(\boldsymbol{\theta})$ is Jacobian transformation matrix and $\boldsymbol{F}_{\mathrm{m}}(\boldsymbol{p},\boldsymbol{l})$ is the static force vector of pneumatic muscles with each component given by (Tondu and Lopez, 2000)

$$F_{\mathrm{m}i}(l_i,p_i)=A(l_i)p_i+F_{\mathrm{r}}(l_i), \tag{2}$$

where $A(l_i)$ and $F_{\mathrm{r}}(l_i)$ are the equivalent cylinder area and rubber elastic force of pneumatic muscle, respectively.

Substitute Eq.(2) into Eq.(1) while noting $\dot{\boldsymbol{l}}=\boldsymbol{J}(\boldsymbol{\theta})\dot{\boldsymbol{\theta}}$, one obtains

$$\ddot{\boldsymbol{l}}=\boldsymbol{H}_{\mathrm{a}}(\boldsymbol{\theta})\boldsymbol{A}_{\mathrm{c}}(\boldsymbol{l})\boldsymbol{p}+\boldsymbol{H}_{\mathrm{b}}(\boldsymbol{\theta},\dot{\boldsymbol{\theta}})+\boldsymbol{d}_{\mathrm{l}}, \tag{3}$$

where

$$\boldsymbol{H}_{\mathrm{a}}(\boldsymbol{\theta})=\boldsymbol{J}(\boldsymbol{\theta})\boldsymbol{M}^{-1}(\boldsymbol{\theta})\boldsymbol{J}^{\mathrm{T}}(\boldsymbol{\theta}),$$
$$\boldsymbol{A}_{\mathrm{c}}(\boldsymbol{l})=\mathrm{diag}\left(A(l_1),A(l_2),A(l_3)\right),$$
$$\boldsymbol{H}_{\mathrm{b}}(\boldsymbol{\theta})=\boldsymbol{J}(\boldsymbol{\theta})\boldsymbol{M}^{-1}(\boldsymbol{\theta})\boldsymbol{J}^{\mathrm{T}}(\boldsymbol{\theta})\boldsymbol{F}_{\mathrm{r}}(\boldsymbol{l})+\dot{\boldsymbol{J}}(\boldsymbol{\theta},\dot{\boldsymbol{\theta}})\dot{\boldsymbol{\theta}}-\boldsymbol{J}(\boldsymbol{\theta})\boldsymbol{M}^{-1}(\theta)\left[\boldsymbol{C}(\boldsymbol{\theta},\dot{\boldsymbol{\theta}})\dot{\boldsymbol{\theta}}+\boldsymbol{G}(\boldsymbol{\theta})+\boldsymbol{J}^{\mathrm{T}}\boldsymbol{F}_{\mathrm{f}}(\boldsymbol{l},\dot{\boldsymbol{l}},\boldsymbol{p})\right],$$
$$\boldsymbol{d}_{\mathrm{l}}=-\boldsymbol{J}(\boldsymbol{\theta})\boldsymbol{M}^{-1}(\boldsymbol{\theta})\boldsymbol{d}_{\mathrm{t}}.$$

Eq.(3) is a MIMO dynamics and there exist coupling effects between the pressures and the contractive accelerations of different driving units. To remove such coupling effects, a SISO decoupling dynamics in task-space is proposed as follows for each driving unit i:

$$\ddot{l}_i=f_{\mathrm{a}}(\boldsymbol{\theta})A(l_i)p_i+f_{\mathrm{b}}(\boldsymbol{\theta},\dot{\boldsymbol{\theta}})+d_{xi}, \tag{4}$$

where $f_{\mathrm{a}}(\boldsymbol{\theta})$ is the ith principal diagonal element of matrix $\boldsymbol{H}_{\mathrm{a}}(\boldsymbol{\theta})$, $f_{\mathrm{b}}(\boldsymbol{\theta},\dot{\boldsymbol{\theta}})$ is the ith element of $\boldsymbol{H}_{\mathrm{b}}(\boldsymbol{\theta},\dot{\boldsymbol{\theta}})$, and d_{xi} is the lumped disturbance including the disturbance of the ith driving unit and the coupling effects of the other two driving units.

Simplified model in muscle-space

The pressure dynamics of each driving unit is (Zhu *et al.*, 2006)

$$\dot{p}_i=-\frac{\lambda_{\mathrm{a}i}(p_i+p_0)\dot{V}_i}{V_i}+\frac{\lambda_{\mathrm{b}i}RT_iq_{\mathrm{m}i}}{V_i}+d_{\mathrm{m}i}, \tag{5}$$

where $\lambda_{\mathrm{a}i}$ and $\lambda_{\mathrm{b}i}$ are the polytropic exponents, p_0 the atmospheric pressure, V_i the pneumatic muscle's inner volume, R the gas constant, T_i the thermodynamic temperature of pneumatic muscle, $d_{\mathrm{m}i}$ the disturbance in muscle-space, and $q_{\mathrm{m}i}$ the mass flow rate of air through the valve given by

$$q_{\mathrm{m}i}=u_i\chi_i(p_{\mathrm{u}i},p_{\mathrm{d}i},T_{\mathrm{u}i}), \tag{6}$$

where u_i is the duty cycle and χ_i is a nonlinear flow gain function, $p_{\mathrm{u}i}$ and $p_{\mathrm{d}i}$ are the upstream pressure and downstream pressure respectively, and $T_{\mathrm{u}i}$ is the upstream temperature.

Considering that the pressure information of pneumatic muscle must be provided in the process of designing the controller while the pressure could not be obtained by measurement in the absence of pressure sensors, the model-based pressure observer should be constructed according to Eqs.(5) and (6). However, since Eq.(6) is a nonlinear function of the unmeasured pressure, Eqs.(5) and (6) cannot be directly used to design the pressure observer. Hence, assuming the flow rate gain function $\chi_i(p_{\mathrm{u}i},p_{\mathrm{d}i},T_{\mathrm{u}i})$ to be constant and merging Eq.(6) with Eq.(5), a simplified model in muscle-space could be expressed as Eq.(7), which is a linear function of the unmeasured pressure:

$$\dot{p}_i=g_{\mathrm{a}}(l_i)u+g_{\mathrm{b}}(l_i)\dot{l}_ip_i+g_{\mathrm{c}}(l_i)\dot{l}_i+d_{\mathrm{p}i}, \tag{7}$$

where $g_{\mathrm{a}}(l_i)$, $g_{\mathrm{b}}(l_i)$ and $g_{\mathrm{c}}(l_i)$ are nonlinear functions of contractive length of pneumatic muscles:

$$g_{\mathrm{a}}(l_i)=\frac{\lambda_{\mathrm{b}i}RT_i\chi_i}{V(l_i)},\quad g_{\mathrm{b}}(l_i)=-\frac{\lambda_{\mathrm{a}i}}{V(l_i)}\frac{\partial V(l_i)}{\partial l_i},$$
$$g_{\mathrm{c}}(l_i)=-\frac{\lambda_{\mathrm{a}i}p_0}{V(l_i)}\frac{\partial V(l_i)}{\partial l_i},$$

and $d_{\mathrm{p}i}$ is the model error during simplification which will be attenuated by robust feedback term.

SISO dynamics in state-space

For each driving unit, state variables are defined as $\boldsymbol{x}=[l_i,\dot{l}_i,p_i]^{\mathrm{T}}$ (i=1,2,3). According to Eqs.(4) and (7), the following SISO dynamics in state-space can be obtained:

$$\begin{cases}\dot{x}_1=x_2,\\ \dot{x}_2=f_{\mathrm{a}}(\boldsymbol{\theta})A(x_1)x_3+f_{\mathrm{b}}(\boldsymbol{\theta},\dot{\boldsymbol{\theta}})+d_{\mathrm{x}},\\ \dot{x}_3=g_{\mathrm{a}}(x_1)u+g_{\mathrm{b}}(x_1)x_2x_3+g_{\mathrm{c}}(x_1)x_2+d_{\mathrm{p}}.\end{cases} \tag{8}$$

PROBLEMS TO BE ADDRESSED

The nonlinear disturbances in task-space and muscle-space can be decomposed into unknown constant nominal values and time-varying uncertainties, i.e., $d_{\mathrm{x}}=d_{\mathrm{x0}}+\tilde{d}_{\mathrm{x}}$, $d_{\mathrm{p}}=d_{\mathrm{p0}}+\tilde{d}_{\mathrm{p}}$. Let $\boldsymbol{\beta}$ be the unknown parameter vector, $\hat{\boldsymbol{\beta}}$ the estimate of $\boldsymbol{\beta}$ and $\tilde{\boldsymbol{\beta}}=\hat{\boldsymbol{\beta}}-\boldsymbol{\beta}$ the estimation error.

Assumption 1 The x_3-subsystem in Eq.(8) with x_3 as the state and u, x_1, x_2 as the inputs, is bounded-input-bounded-state stable in the sense that for every $x_{30}\in\mathbb{R}$ and every $u, x_1, x_2 \in L_\infty^1[0,\infty)$, the solution x_3 starting from the initial condition x_{30} is bounded, i.e., $x_3(t) \in L_\infty^1[0,\infty)$ (Yao and Xu, 2001) .

Assumption 2 The extents of the parametric uncertainties and nonlinear uncertainties are known, i.e.,

$$\boldsymbol{\beta} \in \Omega_{\boldsymbol{\beta}} = \left\{ \boldsymbol{\beta} : \boldsymbol{\beta}_{\min} \le \boldsymbol{\beta} \le \boldsymbol{\beta}_{\max} \right\},$$
$$|\tilde{\boldsymbol{d}}_{\mathrm{x}}| \le \boldsymbol{d}_{\mathrm{xmax}},\ |\tilde{\boldsymbol{d}}_{\mathrm{p}}| \le \boldsymbol{d}_{\mathrm{pmax}},$$

where $\boldsymbol{\beta}_{\max}=[\boldsymbol{\beta}_{1\max},\ldots,\boldsymbol{\beta}_{n\max}]^{\mathrm{T}}$ is the maximum parameter vector and $\boldsymbol{\beta}_{\min}=[\boldsymbol{\beta}_{1\min},\ldots,\boldsymbol{\beta}_{n\min}]^{\mathrm{T}}$ is the minimum parameter vector, $\boldsymbol{d}_{\mathrm{xmax}}$ and $\boldsymbol{d}_{\mathrm{pmax}}$ are known vectors.

Parameter projection

A discontinuous projection can be defined as Eq.(9) in order to guarantee that the parameter estimates given by Eq.(10) remain in the known bounded region all the time (Yao and Tomizuka, 1997).

$$Proj_{\hat{\boldsymbol{\beta}}}(\delta_i)=\begin{cases} 0, & \hat{\boldsymbol{\beta}}_i = \boldsymbol{\beta}_{i\max} \text{ and } \delta_i > 0, \\ 0, & \hat{\boldsymbol{\beta}}_i = \boldsymbol{\beta}_{i\min} \text{ and } \delta_i < 0, \\ \delta_i, & \text{otherwise.} \end{cases} \tag{9}$$

The adaptation law is given by

$$\dot{\hat{\boldsymbol{\beta}}} = Proj_{\hat{\boldsymbol{\beta}}}(\boldsymbol{\Gamma\sigma}), \tag{10}$$

where $\boldsymbol{\Gamma}>\boldsymbol{0}$ is a diagonal matrix and $\boldsymbol{\sigma}$ is an adaptation function to be synthesized later. It can be shown that for any adaptation function, the projection mapping used in Eq.(10) guarantees

$$\left.\begin{aligned} &\text{(P1)}\ \hat{\boldsymbol{\beta}} \in \Omega_{\boldsymbol{\beta}} = \{\hat{\boldsymbol{\beta}}: \boldsymbol{\beta}_{\min} \le \hat{\boldsymbol{\beta}} \le \boldsymbol{\beta}_{\max}\}, \\ &\text{(P2)}\ \tilde{\boldsymbol{\beta}}^{\mathrm{T}}[\boldsymbol{\Gamma}^{-1}Proj_{\hat{\boldsymbol{\beta}}}(\boldsymbol{\Gamma\sigma}) - \boldsymbol{\sigma}] \le \boldsymbol{0},\ \forall \boldsymbol{\sigma}. \end{aligned}\right\} \tag{11}$$

Difficulties in designing observer/controller

For trajectory tracking control of the parallel manipulator driven by pneumatic muscles without the need of measuring pressures, the main difficulties are analyzed as follows.

(1) Due to the nonlinearities of robotic dynamics, pressure dynamics and flow rate characteristics, the unmeasured pressure could not be accurately represented by other measured state variables in linear form. Thus, it is impossible to design a linear pressure observer based on the accurate model (Brogan, 1985).

(2) It must be noted that there exist large uncertainties in the system dynamics, such as the parametric uncertainties from modeling the static force and the friction force of pneumatic muscle, the nonlinear uncertainties from simplifying pressure dynamics of pneumatic muscle and flow characteristic of fast switching valves and the coupling effects of MIMO dynamics, and the dynamic uncertainties from estimating the unmeasured pressures. The above uncertainties could not be attenuated only by robust observer-controller method (Tarek and Francoise, 1999). Therefore, an adaptive robust observer-controller method should be adopted for compensating and attenuating these uncertainties.

(3) The model uncertainties are mismatched, i.e., both parametric uncertainties and nonlinear uncertainties appear in the dynamic equations that are not directly related to the control input u. Therefore the backstepping design technology should be employed to overcome the design difficulties for achieving asymptotic stability (Bu and Yao, 2001).

PRESSURE ESTIMATATION

Define a variable as follows (Yao and Xu, 2001):

$$\zeta = x_3 - \omega(x_1, x_2), \tag{12}$$

where $\omega(x_1,x_2)$ is a design function yet to be determined. From Eq.(8), the derivative of Eq.(12) is

$$\dot{\zeta} = g_{\mathrm{a}}(x_1)u + \left[g_{\mathrm{b}}(x_1)x_2 - \frac{\partial\omega}{\partial x_2} f_{\mathrm{a}}(\boldsymbol{\theta})A(x_1) \right](\zeta + \omega) +$$
$$g_{\mathrm{c}}(x_1)x_2 + d_{\mathrm{p}} - \frac{\partial\omega}{\partial x_1}x_2 - \frac{\partial\omega}{\partial x_2} f_{\mathrm{b}}(\boldsymbol{\theta},\dot{\boldsymbol{\theta}}) - \frac{\partial\omega}{\partial x_2}d_{\mathrm{x}}. \tag{13}$$

For simplicity, let

$$\begin{cases} A_\zeta = g_{\mathrm{b}}(x_1)x_2 - \dfrac{\partial\omega}{\partial x_2} f_{\mathrm{a}}(\boldsymbol{\theta})A(x_1),\ \zeta_{\eta01} = g_{\mathrm{a}}(x_1)u, \\ \zeta_{\eta02} = A_\zeta\omega + g_{\mathrm{c}}(x_1)x_2 - \dfrac{\partial\omega}{\partial x_1}x_2 - \dfrac{\partial\omega}{\partial x_2} f_{\mathrm{b}}(\boldsymbol{\theta},\dot{\boldsymbol{\theta}}), \\ \zeta_{\eta1} = -\dfrac{\partial\omega}{\partial x_2},\quad \zeta_{\eta2} = 1. \end{cases} \tag{14}$$

Then, Eq.(13) is rewritten as

$$\dot{\zeta} = A_\zeta \zeta + \zeta_{\eta 01} + \zeta_{\eta 02} + \zeta_{\eta 1} d_{x0} + \zeta_{\eta 2} d_{p0} + \zeta_{\eta 1} \tilde{d}_x + \zeta_{\eta 2} \tilde{d}_p. \tag{15}$$

If d_{x0} and d_{p0} were known, a nonlinear observer would be designed as

$$\dot{\hat{\zeta}} = A_\zeta \hat{\zeta} + \zeta_{\eta 01} + \zeta_{\eta 02} + \zeta_{\eta 1} d_{x0} + \zeta_{\eta 2} d_{p0}. \tag{16}$$

Then, the state estimation error $\tilde{\zeta} = \hat{\zeta} - \zeta$ would be governed by the following dynamic system:

$$\dot{\tilde{\zeta}} = A_\zeta \tilde{\zeta} - \Delta_1, \tag{17}$$

where

$$\Delta_1 = \zeta_{\eta 1} \tilde{d}_x + \zeta_{\eta 2} \tilde{d}_p.$$

Since d_{x0} and d_{p0} are unknown, the observer Eq.(16) is not implementable, but it provides motivation for the design of the following nonlinear filters:

$$\begin{cases} \dot{\zeta}_{\theta 01} = A_\zeta \zeta_{\theta 01} + \zeta_{\eta 01}, & \dot{\zeta}_{\theta 02} = A_\zeta \zeta_{\theta 02} + \zeta_{\eta 02}, \\ \dot{\zeta}_{\theta 1} = A_\zeta \zeta_{\theta 1} + \zeta_{\eta 1}, & \dot{\zeta}_{\theta 2} = A_\zeta \zeta_{\theta 2} + \zeta_{\eta 2}. \end{cases} \tag{18}$$

The pressure estimation can thus be represented by

$$\hat{\zeta} = \zeta_{\theta 01} + \zeta_{\theta 02} + \zeta_{\theta 1} d_{x0} + \zeta_{\theta 2} d_{p0}. \tag{19}$$

From Eqs.(18) and (19), it can be verified that the observer error dynamics is still described by Eq.(17). Therefore, the unmeasured pressure is

$$x_3 = \zeta_{\theta 01} + \zeta_{\theta 02} + \zeta_{\theta 1} d_{x0} + \zeta_{\theta 2} d_{p0} + \omega - \tilde{\zeta}. \tag{20}$$

Let $A_\zeta=-k$ ($k>0$) such that the unperturbed system of observer error dynamics is exponentially stable, i.e., when $\Delta_1 = 0$, the observation error $\tilde{\zeta}$ converges to zero exponentially. Thus, from Eq.(14), $\omega(x_1,x_2)$ is obtained.

$$\omega(x_1, x_2) = n_a^{-1}(\boldsymbol{\theta}, x_1)[g_b(x_1) x_2^2 / 2 + k x_2], \tag{21}$$

where $n_a(\boldsymbol{\theta},x_1)=f_a(\boldsymbol{\theta})A(x_1)$ is a positive function.

Hence, according to Assumption 1, the observation error would be bounded.

ADAPTIVE ROBUST CONTROLLER DESIGN

A discontinuous projection based adaptive robust controller integrated with the above pressure observer is developed to accomplish the high precision posture trajectory tracking of the parallel manipulator with dynamic uncertainties (Yao and Tomizuka, 1997; Yao and Xu, 2001). The procedure of backstepping design is illustrated as follows.

Step 1: Define a switching-function-like quantity as

$$z_2 = \dot{z}_1 + k_c z_1, \tag{22}$$

where $z_1=x_1-x_{1d}$ is the trajectory tracking error and k_c is a positive feedback constant. If z_2 converges to a small value or zero, then z_1 will converge to a small value or zero since the transfer function from z_2 to z_1 is stable. Substituting Eqs.(8) and (20) into Eq.(22), z_2 dynamics is

$$\begin{aligned} \dot{z}_2 = {} & n_a \zeta_{\theta 01} + n_a \zeta_{\theta 02} + (n_a \zeta_{\theta 1} + 1) d_{x0} + n_a \zeta_{\theta 2} d_{p0} \\ & + n_a \omega - n_a \tilde{\zeta} + f_b - \ddot{x}_d + k_c \dot{e}. \end{aligned} \tag{23}$$

For the purpose of z_2 converging to zero, define the unknown parameters in task-space as $\boldsymbol{\beta}_2=[d_{x0},d_{p0}]^T$ and the virtual input as $v=\zeta_{\theta 01}$. Then, the regressor for parameter adaptation is $\boldsymbol{\varphi}_2=[n_a\zeta_{\theta 1}+1, n_a\zeta_{\theta 2}]^T$. And $\hat{\boldsymbol{\beta}}_2$ is updated by $\dot{\hat{\boldsymbol{\beta}}}_2 = Proj_{\hat{\beta}}(\boldsymbol{\Gamma}_2 \boldsymbol{\sigma}_2)$ with the parameter adaptation function given by $\boldsymbol{\sigma}_2 = \boldsymbol{\varphi}_2 z_2$.

The desired virtual input consists of two terms:

$$v_d = v_{da} + v_{ds}, \tag{24a}$$

$$v_{da} = n_a^{-1}[-n_a \zeta_{\theta 02} - n_a \omega - f_b + \ddot{x}_d - k_c \dot{e} - \boldsymbol{\varphi}_2^T \hat{\boldsymbol{\beta}}_2], \tag{24b}$$

where v_{da} functions as the adaptive control part used to achieve an improved model compensation, and v_{ds} is a robust control law including the following two terms:

$$v_{ds} = v_{ds1} + v_{ds2}, \quad v_{ds1} = -n_a^{-1} k_2 z_2, \tag{25}$$

where k_2 is a positive definite control gain, v_{ds2} is synthesized to dominate the model uncertainties coming from both parametric uncertainties and nonlinear uncertainties, which is chosen to satisfy the following conditions:

$$\begin{cases} z_2(n_a v_{ds2} - \boldsymbol{\varphi}_2^{T}\tilde{\boldsymbol{\beta}}_2 - n_a\tilde{\zeta}) \le \varepsilon_2, \\ z_2 v_{ds2} \le 0, \end{cases} \tag{26}$$

where ε_2 is a positive design parameter.

Define the positive semi-definite (p.s.d) function $V_2 = z_2^2/2$ and denote the input discrepancy as $z_3=v-v_d$. From Eqs.(23) and (24), the time derivative of V_2 is

$$\dot{V}_2 = -k_2 z_2^2 + z_2[-\boldsymbol{\varphi}_2^{T}\tilde{\boldsymbol{\beta}}_2 + n_a z_3 - n_a\tilde{\zeta} + n_a v_{ds2}]. \tag{27}$$

Step 2: Synthesize a control input u so that z_3 converges to zero or a small value with a guaranteed transient performance.

The time derivative of z_3 is given by Eq.(28) while noting Eqs.(14), (18) and (24):

$$\dot{z}_3 = A_\varsigma \zeta_{\theta01} + g_a u - \dot{v}_{dc} - \dot{v}_{du}, \tag{28}$$

where

$$\dot{v}_{dc} = \frac{\partial v_d}{\partial x_1}\hat{x}_2 + \frac{\partial v_d}{\partial x_2}\hat{\dot{x}}_2 + \frac{\partial v_d}{\partial \omega}\left(\frac{\partial \omega}{\partial x_1}\hat{x}_2 + \frac{\partial \omega}{\partial x_2}\hat{\dot{x}}_2\right) + \frac{\partial v_d}{\partial \zeta_{\theta02}}\dot{\zeta}_{\theta02} + \frac{\partial v_d}{\partial \zeta_{\theta1}}\dot{\zeta}_{\theta1} + \frac{\partial v_d}{\partial \zeta_{\theta2}}\dot{\zeta}_{\theta2} + \frac{\partial v_d}{\partial \hat{\boldsymbol{\beta}}_2}\dot{\hat{\boldsymbol{\beta}}}_2 + \frac{\partial v_d}{\partial t},$$

and

$$\dot{v}_{du} = \left(\frac{\partial v_d}{\partial x_1} + \frac{\partial v_d}{\partial \omega}\frac{\partial \omega}{\partial x_1}\right)(x_2 - \hat{x}_2) + \left(\frac{\partial v_d}{\partial x_2} + \frac{\partial v_d}{\partial \omega}\frac{\partial \omega}{\partial x_2}\right)(\dot{x}_2 - \hat{\dot{x}}_2),$$

where $\hat{x}_2$ and $\hat{\dot{x}}_2$ are deduced from x_1 by a second-order differential filter (Zhu *et al.*, 2006). Note that $\dot{v}_{dc}$ represents the calculable part of $\dot{v}_d$ and can be used to design control functions, but $\dot{v}_{du}$ can not due to various uncertainties.

To attenuate the effect of $\dot{v}_{du}$, let $\dot{v}_{du}$ be decomposed into a constant nominal value and time-varying uncertainties, i.e., $\dot{v}_{du} = d_{v0} + \tilde{d}_v$. For the purpose of z_3 converging to zero or a small value with a guaranteed performance, define the unknown parameter in muscle-space as $\boldsymbol{\beta}_3=d_{v0}$. Then, the regressor for parameter adaptation is $\boldsymbol{\varphi}_3=1$. And $\hat{\boldsymbol{\beta}}_3$ is updated by $\dot{\hat{\boldsymbol{\beta}}}_3 = Proj_{\hat{\beta}}(\boldsymbol{\Gamma}_3\boldsymbol{\sigma}_3)$ with the parameter adaptation function given by $\boldsymbol{\sigma}_3=-\boldsymbol{\varphi}_3 z_3$.

The desired control input consists of two terms:

$$u = u_{da} + u_{ds},\ u_{da} = g_a^{-1}(-A_\varsigma\zeta_{\theta01} + \dot{v}_{dc} - n_a z_3 + \hat{d}_{v0}), \tag{29}$$

where u_{da} is used for adaptive model compensation and the robust control law u_{ds} consists of the following two terms:

$$u_{ds} = u_{ds1} + u_{ds2},\ u_{ds1} = -g_a^{-1}k_3 z_3, \tag{30}$$

where k_3 is a positive feedback gain, u_{ds2} is a robust control function chosen to satisfy the following conditions to dominate all model uncertainties:

$$\begin{cases} z_3(g_a u_{ds2} + \boldsymbol{\varphi}_3^{T}\tilde{\boldsymbol{\beta}}_3 - \tilde{d}_v) \le \varepsilon_3, \\ z_3 u_{ds2} \le 0, \end{cases} \tag{31}$$

where ε_3 is a positive design parameter which can be arbitrarily small.

To see how the above control function works, define a p.s.d. function $V_3 = V_2 + z_3^2/2$. The time derivative of V_3, when Eqs.(28) and (29) are substituted into, is

$$\dot{V}_3 = -k_2 z_2^2 - k_3 z_3^2 + z_3[g_a u_{ds2} + \boldsymbol{\varphi}_3^{T}\tilde{\boldsymbol{\beta}}_3 - \tilde{d}_v] + z_2[-\boldsymbol{\varphi}_2^{T}\tilde{\boldsymbol{\beta}}_2 - n_a\tilde{\zeta} + n_a v_{ds2}]. \tag{32}$$

Substituting Eqs.(26) and (31) into Eq.(32), then $\dot{V}_3$ is bounded above by

$$\dot{V}_3 \le -k_2 z_2^2 - k_3 z_3^2 + \varepsilon_2 + \varepsilon_3. \tag{33}$$

The solution of inequality (33) satisfies

$$V_3(t) \le \exp(-\lambda_v t)V_3(0) + \frac{\varepsilon_v}{\lambda_v}[1 - \exp(-\lambda_v t)], \tag{34}$$

where $\lambda_v=2\times\min\{k_2, k_3\}$, $\varepsilon_v=\varepsilon_2+\varepsilon_3$.

The parameters k_2, k_3, ε_2, ε_3 could be designed to guarantee that the tracking error be bounded in a preset ball all the time, whereas, in fact, these parameters are constrained by the bandwidth of the total control system due to unmodeled high frequency dynamics, saturation of control inputs, and sampling frequency of digital implementation, etc.

If after a finite time, $\tilde{d}_{\mathrm{x}}=\tilde{d}_{\mathrm{p}}=\tilde{d}_{\mathrm{v}}=0$, i.e., in the presence of parametric uncertainties and dynamic uncertainties only, then asymptotic output tracking (or zero final tracking error) is also achieved.

RESULTS AND DISCUSSION

The pressure observer based adaptive robust controller (POARC) is implemented on the parallel manipulator driven by pneumatic muscles without pressure sensors. Experimental results are illustrated as follows.

The controller is first tested for a smooth step response with initialized and generated trajectory shown in Fig.2. The estimates of lumped disturbances and pressures are shown in Fig.3. The steady-state errors are $e_{x\mathrm{F}}$=0.03852° and $e_{y\mathrm{F}}$=0.03317° and the maximal absolute values of the tracking errors are $e_{x\mathrm{M}}$=0.93118° and $e_{y\mathrm{M}}$=0.73650°. Despite the fact that there exist rather severe uncertainties in task-space and muscle-space due to model simplification and nonlinearties associated with the pneumatic muscle system, the satisfactory transient performance and excellent steady-state errors could be achieved due to the lumped disturbances and pressures being estimated and the unknown uncertainties being attenuated.

For tracking a sinusoidal posture trajectory (amplitude θ_x=2°, θ_y=5° and period 15 s), response comparison between the POARC without pressure sensors and the adaptive robust controller (ARC) with pressure sensors (Zhu *et al.*, 2006) are shown in Fig.4. The control inputs of POARC are shown in Fig.5, and the estimated pressures and measured pressures are shown in Fig.6. As can be seen from Fig.4, the average tracking errors of POARC are $L_2[e_x]$=0.07146° and $L_2[e_y]$=0.15243°, and the maximal absolute values of the tracking errors are $e_{x\mathrm{M}}$=0.20250° and $e_{y\mathrm{M}}$= 0.44423°. It is obvious that the maximal absolute values of the tracking errors of POARC are a little larger than those of ARC. In Figs.5 and 6, the control inputs and the estimates of pressures are bounded all the time and the movement is smooth without control chattering since the discontinuous projection based adaptive robust controller is adopted. Though there are fairly large errors between estimated pressures and measured pressures, the tracking errors could be always small due to large parametric uncertainties and large dynamic uncertainties being compensated through using POARC.

Fig.7 shows the error responses of the contractive lengths of pneumatic muscles both with POARC and with sliding mode controller (SMC) (Tao *et al.*, 2005) under the condition of tracking the same trajectory

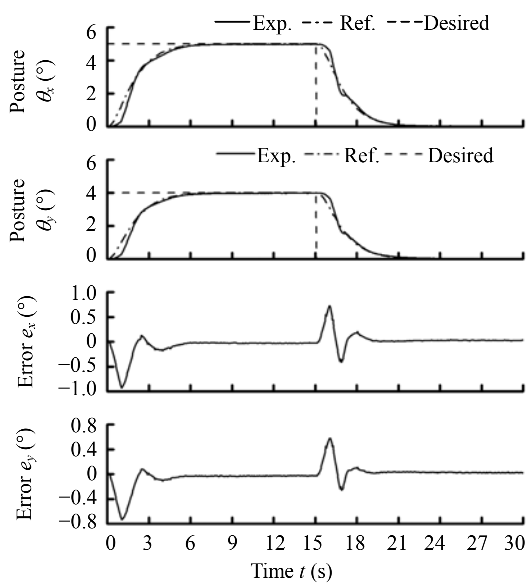

Fig.2 Smooth step response of POARC

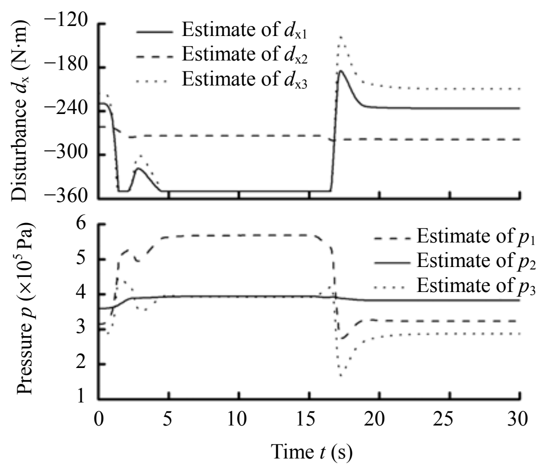

Fig.3 Estimates of disturbance and pressures under smooth step response. d_{xi}, p_i and u_i (i=1,2,3) represent the disturbance, pressure and control input in the ith driving unit, respectively

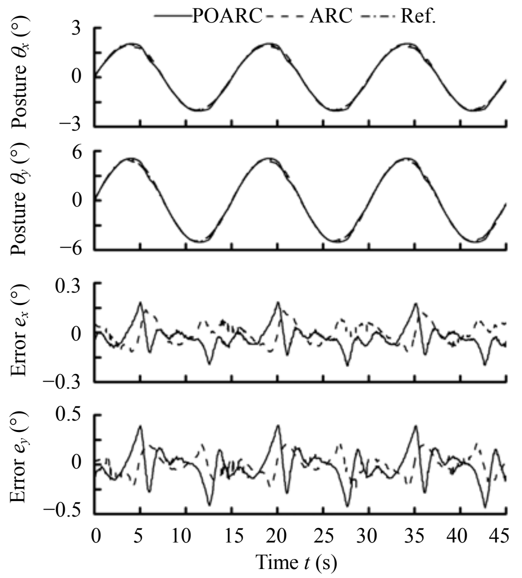

Fig.4 Sinusoidal tracking response of POARC and ARC

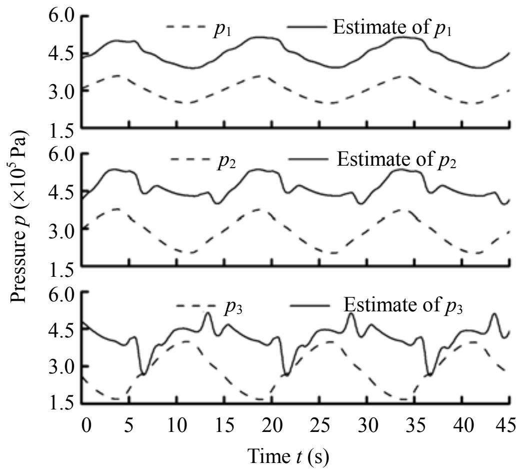

Fig.5 Estimated and measured pressures with POARC under sinusoidal trajectory

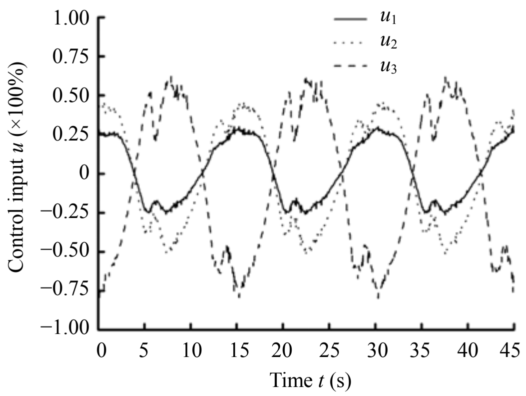

Fig.6 Control inputs of POARC under sinusoidal trajectory

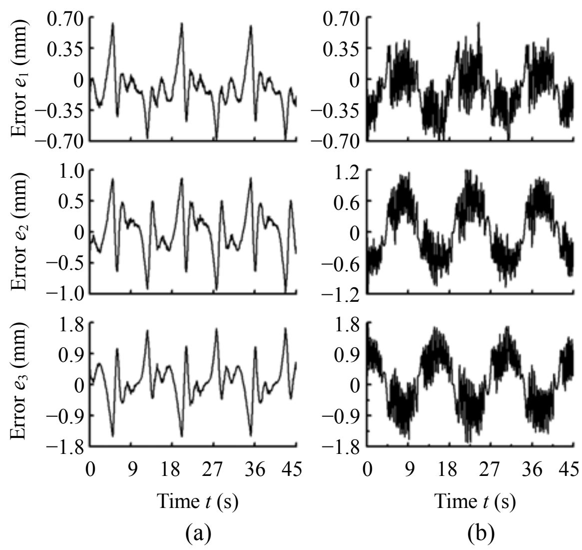

Fig.7 Error comparison of contractive length with (a) POARC and (b) SMC

as above. It must be noted that neither of the two controllers uses pressure sensors. Obviously, the errors of the contractive lengths with SMC in Fig.7 have severe vibration and the parallel manipulator is suffering from vibration all the time since SMC utilizes the tracking errors to design the controller regardless of system model and pressure estimations. Consequently, the fast switching valves switch continuously, which will result in noises of the parallel manipulator and reduce useful life of the fast switching valves. In contrast, POARC makes full use of the available structural information of the unmeasured state dynamics and the prior knowledge about the parameter bounds to design the controller. As a result, small tracking errors with smooth movement and little control chattering are achieved.

For testing the robustness of POARC, the position transducers are given a sudden dither at t=12 s, which can be regarded as a sudden large output disturbance to the system. As can be seen from Fig.8, the system experiences large tracking errors due to the wrong feedback information of position transducers when the dither is introduced. But after the dither disappeared, the system comes back to the stable posture quickly with no fluctuation. This demonstrates the robustness of the proposed control algorithm to disturbances.

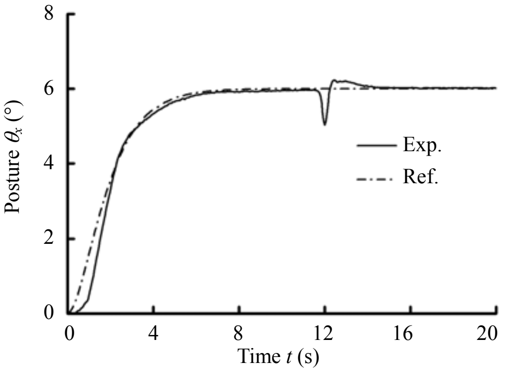

Fig.8 Robustness of POARC to sudden disturbance

CONCLUSION

A nonlinear pressure observer based adaptive robust controller is developed for trajectory tracking control of a parallel manipulator driven by pneumatic muscles without pressure sensors. The nonlinear pressure observer is constructed to recover the unknown states, i.e., pressures on the basis of a SISO decoupling model which is simplified from the actual MIMO coupling model. A robust filter structure is utilized to provide the practical pressure estimation. By integrating the adaptive robust control with the pressure observer, the parametric uncertainties, nonlinear uncertainties coming from model simplification and dynamics uncertainties coming from pressure estimation errors, are effectively compensated and attenuated.

The pressure observer based adaptive robust controller (POARC) is proved to be effective by experimental results. The steady-state errors are less than 0.04° under a smooth step response and the average tracking errors less than 0.16° under a sinusoidal trajectory. Compared with SMC, the proposed POARC performs much better with smooth movement and without control chattering. At the same time, it must be noted that the tracking errors remain small and are not influenced by large estimation errors of the observer.

References

Ahn, K.K., Nguyen, H.T.C., 2007. Intelligent switching control of a pneumatic muscle robot arm using learning vector quantization neural network. *Mechatronics*, **17**: 255-262. [doi:10.1016/j.mechatronics.2006.12.002]

Brogan, W.L., 1985. Modern Control Theory. Prentice-Hall, Englewood Clis, NJ, p.410-420.

Bu, F.P., Yao, B., 2001. Nonlinear Model Based Coordinated Adaptive Robust Control of Electro-hydraulic Robotic Arms via Overparametrizing Method. Proc. IEEE Int. Conf. on Robotics & Automation. Seoul, Korea, p.3459-3464. [doi:10.1109/ROBOT.2001.933153]

Caldwell, D.G., Medrano-Cerda, G.A., Goodwin, M., 1995. Control of pneumatic muscle actuators. *IEEE Control Systems Magazine*, **15**(1):40-48. [doi:10.1109/37.341863]

Costa, N., Caldwell, D.G., 2006. Control of a Biomimetic "Soft-actuated" 10DoF Lower Body Exoskeleton. Proc. First IEEE/RAS-EMBS Int. Conf. on Biomedical Robotics and Biomechatronics. Pisa, Italy, p.495-501. [doi:10.1109/BIOROB.2006.1639137]

Gulati, N., Barth, E.J., 2005. Pressure Observer Based Servo Control of Pneumatic Actuators. Proc. IEEE/ASME Int. Conf. on Advanced Intelligent Mechatronics. Monterey. USA, p.498-503. [doi:10.1109/AIM.2005.1511031]

Hildebrandt, A., Kharitonov, A., Sawodny, O., Gottert, M., Hartmann, A., 2005. On the Zero Dynamic of Servo Pneumatic Actuators and its Usage for Trajectory Planning and Control. Proc. IEEE Int. Conf. on Mechatronics & Automation. Niagara Falls, Canada, p.1241-1246. [doi:10.1109/ICMA.2005.1626731]

Medrano-Cerda, G.A., Bowler, C.J., Caldwell, D.G., 1995. Adaptive Position Control of Antagonistic Pneumatic Muscle Actuators. IEEE/RSJ on Intelligent Robots and Systems. Pittsburgh, USA, p.378-383. [doi:10.1109/IROS.1995.525824]

Nakamura, N., Sekiguchi, M., Kawashima, K., Fujita, T., Kagawa, T., 2002. Developing a Robot Arm Using Pneumatic Artificial Rubber Muscles. Bath Int. Workshop on Power Transmission and Motion Control. University of Bath, UK, p.365-375.

Pandian, S.R., Takemura, F., Hayakawa, Y., Kawamura, S., 2002. Pressure observer-controller design for pneumatic cylinder actuators. *IEEE/ASME Trans. on Mechatronics*, **7**(4):490-499. [doi:10.1109/TMECH.2002.805624]

Takuma, T., Hosoda, K., 2006. Controlling the walking period of a pneumatic muscle walker. *Int. J. Rob. Res.*, **25**(9): 861-866. [doi:10.1177/0278364906069187]

Tao, G.L., Zhu, X.C., Cao, J., 2005. Modeling and controlling of parallel manipulator joint driven by pneumatic muscles. *Chin. J. Mech. Eng. (En. Ed.)*, **18**(4):537-541.

Tao, G.L., Zhu, X.C., Yao, B., Cao, J., 2007. Adaptive Robust Posture Control of a Pneumatic Muscles Driven Parallel Manipulator with Redundancy. American Control Conference. New York City, USA, p.3408-3413.

Tarek, A.A., Francoise, L.L., 1999. Sliding observer-controller design for uncertain triangular nonlinear systems. *IEEE Trans. on Automatic Control*, **44**(6):1244-1249. [doi:10.1109/9.769383]

Tondu, B., Lopez, P., 2000. Modeling and control of McKibben artificial muscle robot actuators. *IEEE Control Systems Magazine*, **20**(2):15-38. [doi:10.1109/37.833638]

Tsagarakis, N.G., Caldwell, D.G., 2003. Development and control of a 'soft-actuated' exoskeleton for use in physiotherapy and training. *Autonomous Robots*, **15**(1): 21-33. [doi:10.1023/A:1024484615192]

Yao, B., Tomizuka, M., 1997. Adaptive robust control of SISO nonlinear systems in a semi-strict feedback form. *Automatica*, **33**(5):893-900. [doi:10.1016/S0005-1098(96)00222-1]

Yao, B., Xu, L., 2001. Observer-based adaptive robust control of a class of nonlinear systems with dynamic uncertainties. *Int. J. Rob. Nonl. Control*, **11**(4):335-356. [doi:10.1002/rnc.557]

Zhu, X.C., Tao, G.L., 2004. Modeling of a servo platform driven by pneumatic artificial muscles. *J. Zhejiang Univ. (Eng. Sci.)*, **38**(8):537-541 (in Chinese).

Zhu, X.C., Tao, G.L., Cao, J., Yao, B., 2006. Adaptive Robust Posture Control of a Pneumatic Muscles Driven Parallel Manipulator. 4th IFAC Symp. on Mechatronic Systems. Heidelberg, Germany, p.764-769.